

Flow pattern assessment in tubes with wire coil inserts in laminar and transition regimes

A. García ^{a,*}, J.P. Solano ^a, P.G. Vicente ^b, A. Viedma ^a

^a Universidad Politécnica de Cartagena, Departamento de Ingeniería Térmica y de Fluidos, Campus de la Muralla del Mar, 30202 Cartagena, Spain

^b Universidad Miguel Hernández, Departamento de Ingeniería de Sistemas Industriales, Avenida de la Universidad, s/n 03202 Elche, Spain

Received 7 February 2006; received in revised form 14 June 2006; accepted 13 July 2006

Available online 1 September 2006

Abstract

The paper presents an analysis of the flow mechanisms in tubes with wire coils using hydrogen bubble visualization and PIV techniques. Results have been contrasted with experimental data on pressure drop. The relation between the observed flow patterns and the friction factor has been analysed.

The experimental analysis that has been carried out allows one to state that at low Reynolds numbers ($Re < 400$) the flow in tubes with wire coils is basically similar to the flow in smooth tubes. At Reynolds numbers between 500 and 700 and in short pitch wire coils a recirculating flow appears. The insertion of wires coils in a smooth tube accelerates significantly the transition to turbulence. This is produced at Reynolds numbers between 700 and 1000 depending on the wire pitch.

© 2006 Elsevier Inc. All rights reserved.

Keywords: Heat transfer enhancement; Wire coil inserts; Heat exchangers; Turbulence promoters

1. Introduction

Wire coils are a type of inserted elements which present some advantages compared to other enhancement techniques, such as artificial roughness by mechanical deformation. They may be installed in an existing smooth tube heat exchanger. They keep the mechanical strength of the smooth tube. Their installation is easy and their cost is very low.

The insertion of a device such as a wire coil inside a smooth tube produces an increase in the heat transfer due to one or more of the following phenomena:

- Turbulence promotion. Wires attached to the wall cause separation in the flow that increases its turbulence level. They act also as roughness elements mixing up the flow in the viscous sublayer.

- Secondary flow promotion. Many inserted devices induce secondary flows which can favour thermal exchange. Helical wire coils produce a helicoidal flow at the periphery superimposed on the main axial flow. Due to the flow velocity increase and to the appearance of centrifugal forces, convection increases. This favours the convection in heating processes.
- Hydraulic diameter reduction. Any inserted element in a smooth tube will reduce the cross-sectional area increasing the average flow velocity. The wetted perimeter also increases and the hydraulic diameter decreases.

Evidence suggests that depending on the wire coil geometry and on the Reynolds number, two different types of flows can occur: rotating flow and separated flow. The first one occurs at the tube periphery due to the helix angle and affects to a greater or lesser extent the thickness of the flow. A separated flow can occur due to the fluid crossover through the wire.

Most of the experimental works on wire coils focus on the turbulent regime and pay little attention to their

* Corresponding author.

E-mail address: alberto.garcia@upct.es (A. García).

Nomenclature

d	envelope (maximum inner) diameter (m)
e	wire diameter (m)
l_p	length of test section between pressure taps (m)
\dot{m}	mass flow rate (kg s^{-1})
p	helical pitch (m)
ΔP	pressure drop across the test section (Pa)
T	temperature (K)

Dimensionless groups

f	Fanning friction factor
Re	Reynolds number

Greek symbols

α	helical angle ($\tan(\pi)d/p$)
μ	dynamic viscosity (Pa s)
ρ	fluid density (kg m^{-3})

Subscripts

a	augmented tube (wire coil fitted inside a smooth tube)
in	tube inlet
out	tube outlet
s	smooth tube

behaviour in laminar and transition regimes. It is worth mentioning the experimental studies by [Uttarwar and Raja Rao \(1985\)](#) and [Inaba et al. \(1994\)](#) and the state-of-the-art reviews carried out by [Wang and Sundén \(2002\)](#) and most recently by [Dewan et al. \(2004\)](#).

An aspect to point out in the analysis of the enhancement techniques is the general ignorance in relation to the physical flow nature. The flow pattern is responsible for heat transfer enhancement and knowledge of it is very useful to optimize the geometry of enhancement techniques. Only the work by [Li et al. \(1982\)](#) on corrugated tubes and the work by [Ravigururajan and Bergles \(1994\)](#) on wire coils have paid attention to this important field of study. [Ravigururajan and Bergles \(1994\)](#) considered their own paper as a preliminary work on flow visualization on flow with wire coils. They pointed out the necessity of carrying out more thorough works in order to have quantitative information on how each variable affects the flow pattern and thus better understanding their influence on heat transfer enhancement. They consider that every type of artificial roughness disturbs the flow in a similar way. Therefore the conclusions for one improvement technique can be extrapolated to another one.

Previous works published on corrugated tubes ([Vicente et al., 2004](#)), on dimpled tubes ([Vicente et al., 2002](#)) and wire coils ([García et al., 2005](#)) suggest that each geometry generates a particular flow pattern as different transitions to turbulence in each technique shows. We consider the suggestion that every artificial roughness disturbs the flow in a similar way to be a simplification that must be handled with extreme care.

The experimental work carried out by the authors with wire coils ([García et al., 2005](#)) showed that transitional flow in tubes with wire coil inserts is produced gradually, and in a different way to that produced in smooth tubes or even in mechanically deformed tubes. That study was centred on establishing thermohydraulic behaviour in wire coils and developing design correlations for pressure drop and heat transfer. The results of that work were complete for design purposes but failed to provide a relation between flow

characteristics and pressure drop and heat transfer augmentation.

This paper studies flow mechanisms by visualization techniques in tubes with wire coils. The visualization results show different flow patterns depending on the Reynolds number. These results are contrasted with experimental data on pressure drop and show their interrelation.

2. Experimental programme

2.1. Visualization facility

The facility depicted in [Fig. 1](#) was built in order to study the flow pattern induced by a wire coil inserted in a tube. The main section consists of a 32 mm diameter acrylic tube

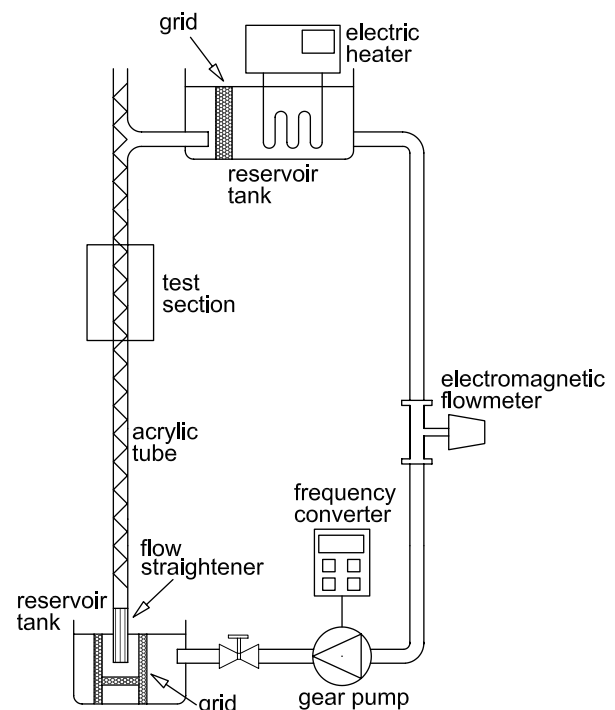


Fig. 1. Visualization facility.

installed between two reservoir tanks, that stabilize the flow. In the upper reservoir tank the flow temperature is regulated by an electric heater and a thermostat. The flow is impelled from the lower calm deposit to the upper one by a gear pump, which is regulated by a frequency converter. By using mixtures of water and propyleneglycol at temperatures from 20 °C to 50 °C, Reynolds numbers between 100 and 20 000 can be obtained. The tests presented in this work were carried out employing a mixture of 50% water and propyleneglycol at temperatures from 25 °C to 40 °C, yielding Reynolds number in the range from 200 to 3000. Heat losses in the vertical tube were calculated and it was confirmed that the velocity field was not modified by buoyancy forces in any test.

The test section has been placed at a distance of 45 diameters from the tube entrance in order to ensure a fully developed flow condition. To improve optical access in this section, a flat-sided acrylic box was placed around the test section. The box was filled with the same test

fluid that flows through the test section. Two different complementary visualization techniques have been used: visualization by hydrogen bubbles and by Particle Image Velocimetry.

The visualization by hydrogen bubbles is a qualitative technique that gives a full perception of the flow, in three-dimensions. Fig. 2 shows a sketch of how this technique has been used. A rear lighting system at 45° has been used.

A copper-wire cathode placed horizontally crosses the tube diameter. By adjusting its feed voltage value, the creation of an appropriate quantity of bubbles for each test was achieved. In order to work with feed voltages below 50 V, the fluid conductivity was increased by adding salt.

Particle Image Velocimetry (PIV) is a well-known technique to obtain global velocity information, instantaneously and with high accuracy. In these experiments planar slices of the flow field that contained the axis of the pipe (longitudinal section) were illuminated, as shown in Fig. 3. The flow was seeded by 50 μ m diameter polyamide particles. The camera viewed the illuminated plane from an orthogonal direction and recorded particle images at two successive instants in time in order to extract the velocity over the planar two-dimensional domain. The spatial resolution of the measurement is 160 μ m/pixel.

A 1 mm thick light sheet is created by a pulsating diode laser of 808 nm wavelength. A computer synchronizes the camera shutter opening and the laser shot at the appropriate frequency for the test conditions.

Image processing was carried out with the software 'vid-PIV', that applies a cross-correlation algorithm between consecutive images. The interrogation window size used for PIV processing was 32×32 pixels, with a 50% overlap. To obtain a clear velocity field, after the images were correlated, a global and a local filter were applied to remove outliers. The resulting vectors were averaged over fifty realizations. Using the standard formula for 20–1 odds, $\pm 1.96\sigma N^{-0.5}$, the uncertainty in PIV measurements is

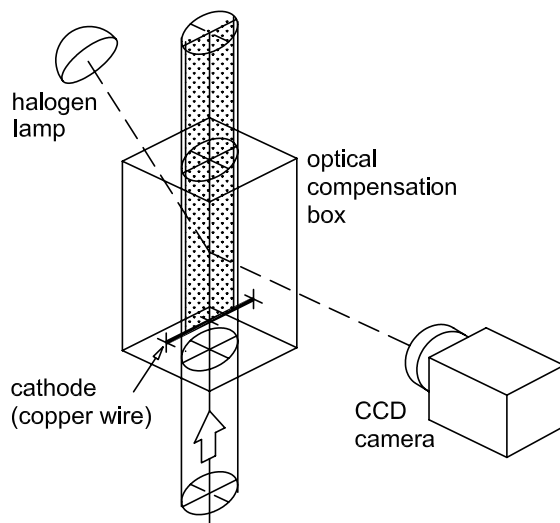


Fig. 2. Sketch of hydrogen bubbles visualization technique.

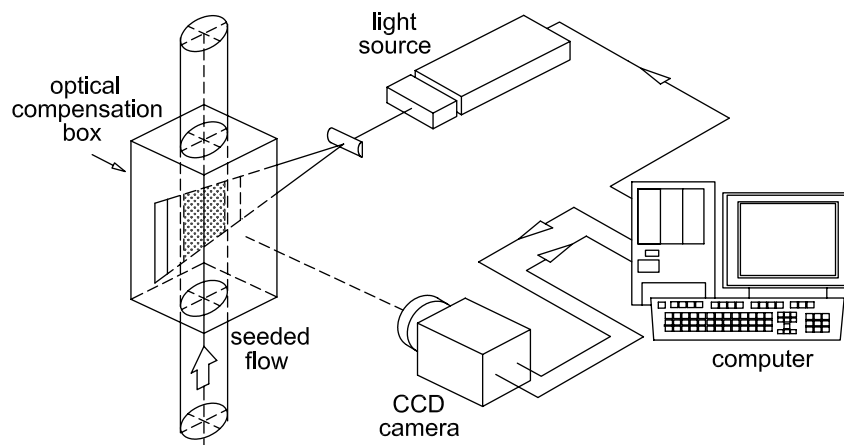


Fig. 3. Sketch of Particle Image Velocimetry (PIV) working principle.

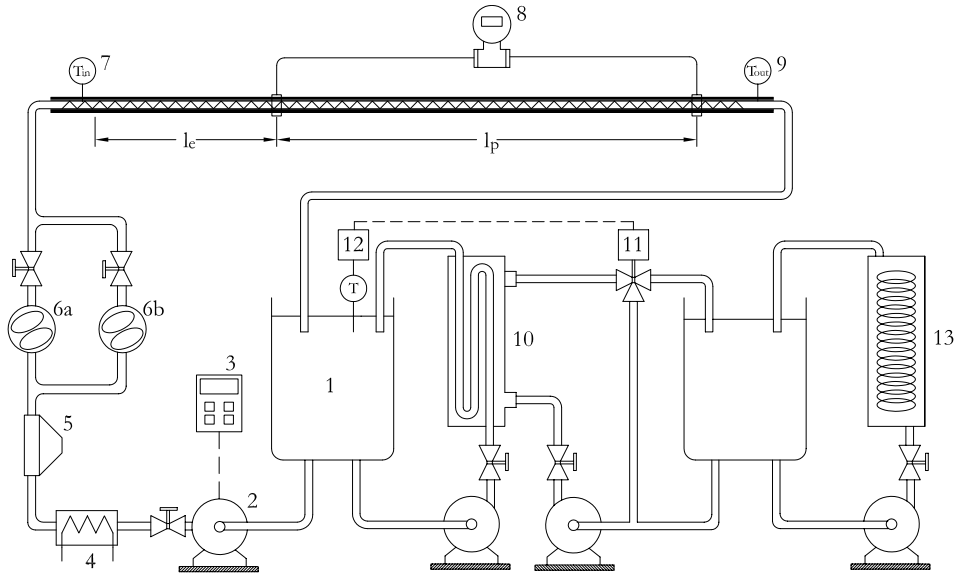


Fig. 4. Experimental setup for pressure drop: (1) reservoir tank; (2) centrifugal pump; (3) frequency converter; (4) electrical heater; (5) coriolis flowmeter; (6) oval wheels flowmeters; (7) fluid inlet temperature; (8) pressure transmitter; (9) fluid outlet temperature; (10) counterflow heat exchanger; (11) regulating valve; (12) PID controller; (13) cooler.

about 3%. Taking into account the uncertainty in the computation of pixels displacements, the final uncertainty in PIV measurement rises to 5%.

2.2. Friction factor measurement tests

A schematic diagram of the experimental setup is shown in Fig. 4. It consisted of two independent circuits: the main circuit where the wire coils were installed and the secondary circuit which was used for regulating the tank temperature to the required value. All the instrumentation was connected to a HP 34970A Data Acquisition Unit.

Fluid inlet and outlet temperatures, T_{in} and T_{out} were measured by submerged type (*Resistance Temperature Detector* (RTDs)). Since the pressure drop tests were carried out in a region under isothermal conditions, the fluid temperature was calculated by $T_f = (T_{in} + T_{out})/2$. The test section length is $l_p = 150$ diameters and is preceded by a hydrodynamic development region of $l_e = 60d$ length. Both test and developing flow regions are insulated in order to ensure isothermal conditions. The inner smooth tube diameter d was used as the reference diameter to calculate all friction factors. Fanning coefficients f were determined from fluid mass flow rate and pressure drop measurements as

$$f = \frac{\Delta P d^5 \pi^2 \rho}{32 l_p \dot{m}^2}. \quad (1)$$

Pressure drop ΔP was measured along the pressure test section ($l_p = 2.88$ m) by means of a highly accurate pressure transducer. Four pressure tappings separated by 90° were coupled to each end of the pressure test section. Two differential pressure transducers of different full scales ensured the accuracy of the experiments.

Experimental uncertainty was calculated by following the “Guide to the expression of uncertainty in measurement” published by ISO (1995). Uncertainty calculations based on a 95% confidence level showed maximum values of 4% for Reynolds number, and 3% for friction factor.

3. Experimental results

An experimental study in three wire coils with the same wire diameter and different non-dimensional pitch has been carried out. Wire coils were produced from a stainless steel coil covered by an ulterior plastic sheet. Table 2 shows the wire coils that have been used in the visualization tests. Since the tube used in the visualization facility has a diameter of 32 mm and the one used in the installation of the pressure drop facility has a diameter of 18 mm, the three wire coils are geometrically similar (Table 1). Therefore, the visualization results can be compared to the pressure drop results.

Tests have allowed the description of different flow patterns and have established with accuracy the Reynolds number at which transition to turbulent flow occurs. The flow will be described in two different areas: the *central region*, which is defined as the tube region that comprises from $r = 0$ to $r = D/2 - e$ and the *peripheral region* placed between $r = D/2 - e$ and $r = D/2$.

Table 1
Geometry of the wire coils tested

	d (mm)	p/d	e/d	p/e	α (deg)
Wire Coil W01	18	1.25	0.076	16.4	68.3
Wire Coil W02	18	1.72	0.076	22.6	61.3
Wire Coil W03	18	3.37	0.076	44.3	43.0

Pressure drop tests.

Table 2
Geometry of the wire coils tested

	d (mm)	p/d	e/d	p/e	α (deg)
Wire Coil W01	32	1.21	0.073	16.6	68.9
Wire Coil W02	32	1.65	0.073	22.6	62.3
Wire Coil W03	32	3.66	0.073	50.1	40.6

Visualization tests.

Before the wire coils were tested, a series of tests was carried out in the smooth tube in order to verify the correct operation of both experimental installations.

3.1. Smooth tube

The flow visualization in a smooth tube by means of the hydrogen bubbles allows one to establish when the flow starts to become unstable and how the transition to the turbulent regime is produced.

Fig. 5 shows the friction factor results obtained under isothermal conditions depending on the Reynolds number. Experimental results in laminar regime are compared with the analytical solution ($f_s = 16/Re$) and results in turbulent regime are compared with the Blasius equation ($f_s = 0.0791 Re^{-0.25}$). Deviations were lower than 4% for the 95% of the experimental data. These tests served to the adjustment and verification of the experimental installation.

Next the results obtained from the hydrogen bubbles visualization along with the pressure drop results are commented:

- **I.** Reynolds number range from 100 to 1800. Stable laminar flow, parabolic velocity profile. Friction factor results adjust perfectly to the curve $f_s = 16/Re$.
- **II.** Reynolds number range from 1800 to 2100. Laminar flow with light flow oscillations. At $Re \approx 2000$ the presence of turbulence outbreaks is appreciated.
- **III.** Reynolds number range higher than 2100. Turbulence is clearly established. From the flow visualization by means of the hydrogen bubbles, the break point at

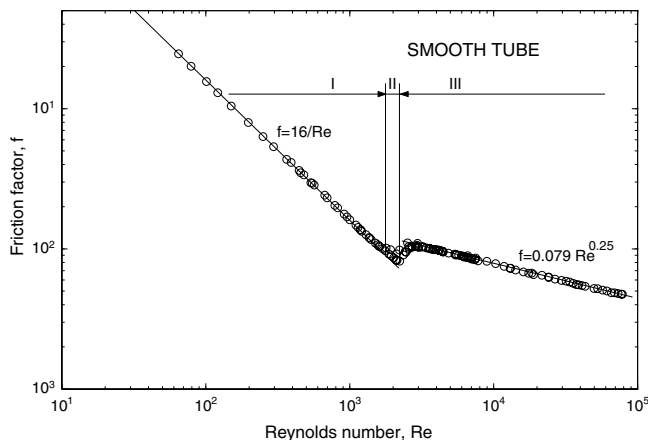


Fig. 5. Fanning friction factor vs. Reynolds number (smooth tube).

$Re = 2100$ was established. In the friction factor curve a minimum at 2100 is observed. Moreover, a quite sudden friction factor increase due to the transition from laminar to turbulent flow is found.

In order to adjust and verify the PIV system, some measurements of the velocity field in the smooth tube were carried out. From the processing of 50 images taken at 100 fps (100 frames per second), the velocity profile that appears in Fig. 6 has been obtained. The velocity profile is made non-dimensional by using the flow average velocity which is calculated by means of the average flow rate in the installation.

The non-dimensional velocity profile achieved adjusts to the theoretical result in most of the tube diameter. The velocity data taken in the nearest region to the wall show deviations. In this region there is light reflection in the tube and it is difficult to measure very low velocities using the PIV technique, since it is based on particle displacement.

3.2. Wire Coil W01, short pitch

The flow characterization in the wire coil has been carried out using the fluid visualization by means of hydrogen bubbles and the velocity profile measurement by the PIV technique. On a qualitative level, images have served to show the flow pattern based on the Reynolds number and to establish the point where transition occurs. The analysis of the general flow structure is carried out simultaneously with the analysis of the friction factor results (Fig. 7).

Four different types of flow structure for the following Reynolds number ranges have been observed:

- **I.** Reynolds numbers from 0 to 350:

This is a stable laminar flow where the fluid in the peripheral region goes through the wire coil without any type of recirculation.

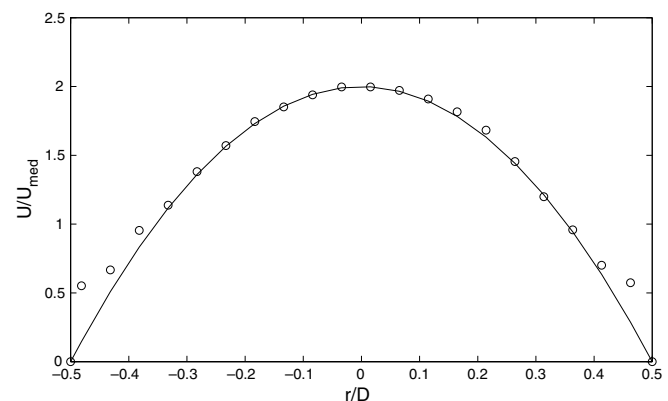


Fig. 6. Velocity profile in the smooth tube obtained by PIV at Reynolds number $Re = 370$.

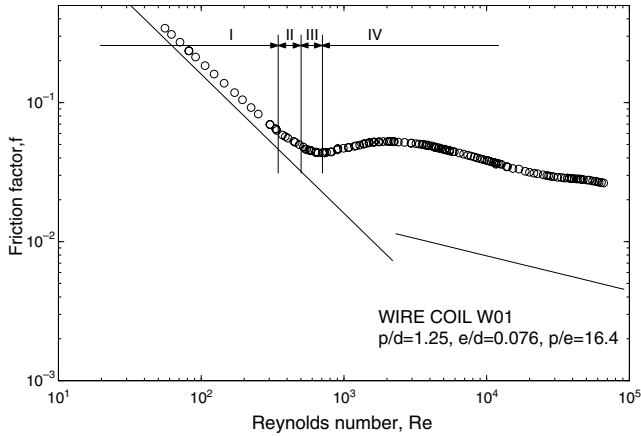


Fig. 7. Fanning friction factor vs. Reynolds number. Wire coil W01 results.

Fig. 8 shows a sketch of the flow pattern at Reynolds numbers below 350. It is observed that in the *peripheral region* ($D/2 - e < r < D/2$) the flow remains attached (separation downstream the wire is not produced).

The flow in the *central region* remains almost unchanged. Visualization by hydrogen bubbles (Fig. 9) shows an ascending stable laminar flow, where there is only an azimuthal velocity component that spins the bubble curtain which is produced by the copper wire. Though it appears that the bubble curtain becomes narrower, it is just a spin of this, as the 2-D and 3-D flow sketches show. The central flow spin depends on the Reynolds number: at $Re = 200$ the central flow spins 90° along 20 diameters whereas at $Re = 350$ the 90° spin occurs along 10 diameters. It can be clearly stated that the flow pattern in the central region is similar to the one that occurs in a smooth tube with a light spin that hardly affects the flow behaviour.

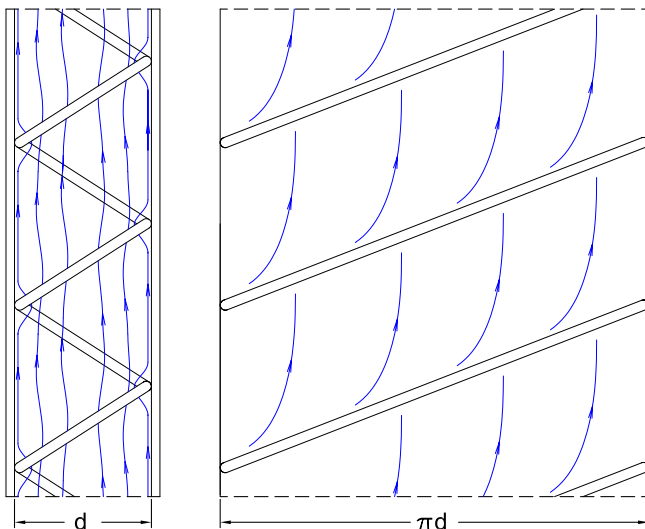


Fig. 8. Flow features for wire coil W01 at $Re < 350$. Left: central flow. Right: flow in the peripheral region.

The wire coil is an inserted element which reduces the tube cross section and increases the average flow velocity. The velocity increases due to the cross section reduction produced by the wire coil is just a 2%, which is practically negligible. Using the PIV technique the velocity field in the central flow region has been measured (Fig. 10). Velocity in the tube axis is 15% higher than which that occurs in a smooth tube without wire coils. Therefore, it can be stated that the wire coil geometry produces an important flow variation, even in the laminar regime.

The variation of the velocity profile shape which the wire coil produces results in a friction factor increase. For Reynolds numbers lower than 350 the friction factor can be correlated by

$$f = 14.5/Re^{0.93}. \quad (2)$$

• II. Reynolds numbers from 350 to 500:

Visualization by hydrogen bubbles shows a stable laminar flow and recirculation downstream of the wire is observed. This recirculation together with the azimuthal velocity component produces a helical flow which ascends along the wire coil body. Fig. 11 shows a sketch of the flow pattern observed: the flow separation downstream the wire observed in the left drawn yields to a helicoical flow in the *peripheral region* ($r = D/2 - e$ to $r = D/2$) represented in the right hand sketch.

The central flow remains laminar and shows a 90° spin along 10 diameters of the tube. Recirculation downstream to the wire produces a perceptible pressure drop increase. In this region the friction factor is proportional to $Re^{-0.55}$ instead Re^{-1} as occurs in the smooth tube. At $Re = 500$, the friction factor is 60% higher to the friction factor in the smooth tube.

• III. Reynolds numbers from 500 to 700:

The general flow topology is similar to that of region II, except that the central flow becomes oscillatory. At $Re = 500$, it is observed that the central flow oscillates and seems to be a laminar undulating flow. At $Re = 600$ flashes of turbulent flow are observed. These are turbulence outbreaks. At $Re = 650$ the central flow is in a turbulent-transitional regime. The flow at the peripheral region follows mostly the helix angle direction. At $Re = 700$ the flow is fully turbulent.

Friction factor becomes almost constant. This means that the pressure drop is proportional to the mean square velocity (a typical solution of turbulent flows). Given the flow structure in the transitional region to turbulence, this is produced smoothly without any kind of discontinuity. In fact, in the pressure drop tests, the transitional point cannot be established (just as occurs in the smooth tube tests).

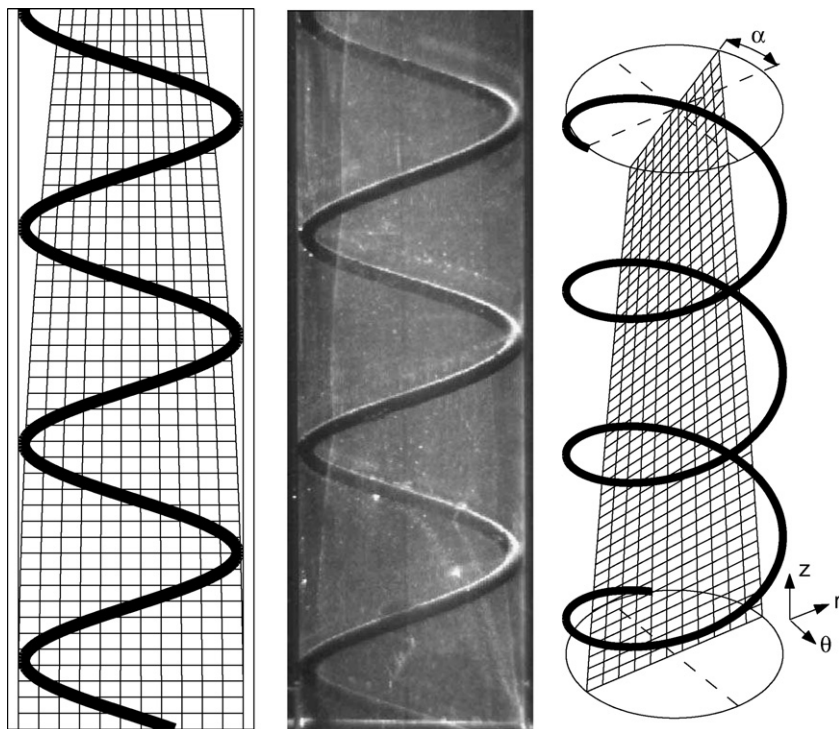


Fig. 9. Central flow for wire coil W01 at $Re < 350$. Visualization by hydrogen bubbles.

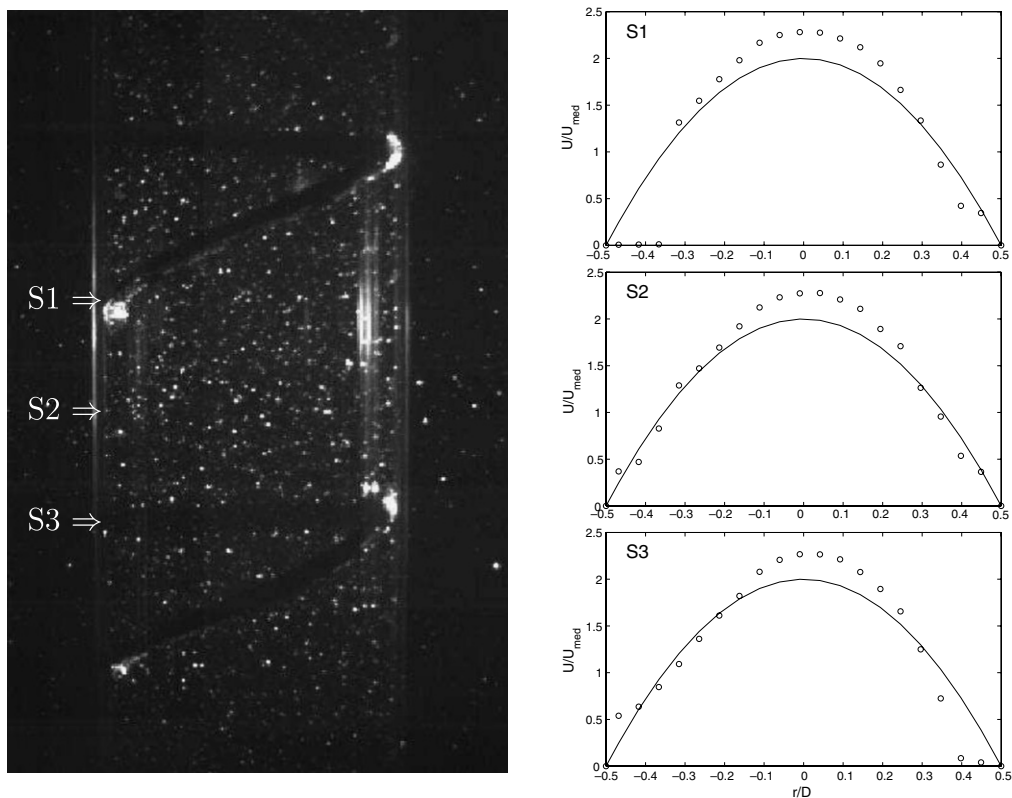


Fig. 10. Flow visualization of wire coil W01 processed by PIV technique.

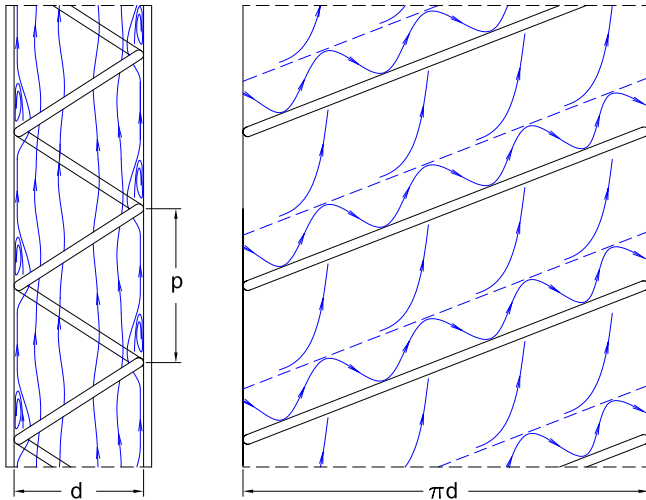


Fig. 11. Flow features for wire coil W01 at $Re = 350$ – 500 . Left: central flow. Right: flow in the peripheral region.

• IV. Reynolds numbers higher than 700:

Turbulence is clearly established. Visualization by hydrogen bubbles shows a strong blend of these and vortex flow structures, typical of turbulent flow. The flow at the peripheral region follows the direction of the wire pitch. Flow observation is difficult due to the strong blend of the peripheral and central flows.

Results make it possible to state that for the same Reynolds number, the turbulence level in a wire coil is much higher than that in a smooth tube. At $Re = 3000$ the friction factor produced by the wire coil W01 is five times higher than that of the smooth tube. From this Reynolds number on, the tendency of the friction factor curve is to follow the typical behaviour of turbulent flow on structured rough surfaces ($f \propto Re^{-0.2}$).

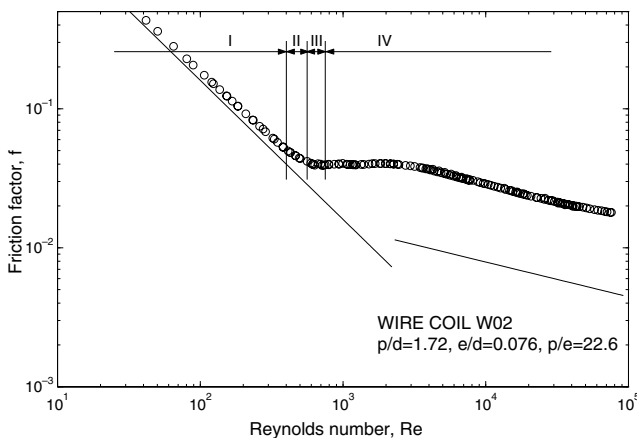


Fig. 12. Fanning friction factor vs. Reynolds number. Wire coil W02 results.

3.3. Wire Coil W02, intermediate pitch

Wire coil W02 has a larger non-dimensional pitch p/d than W01. Features observed in wires W01 and W02 are very similar. In W02 transitions among the different flow patterns occur at slightly higher Reynolds numbers.

Fig. 12 shows results for the pressure drop at Reynolds numbers between 50 and 70 000. Next, results for the friction factor together with visualization results for the following Reynolds numbers range are commented upon:

• I. Reynolds numbers lower than 400:

Stable laminar flow. The flow in the wire region passes over the wire without any type of recirculation. A small increase in the friction factor is obtained. This can be correlated by:

$$f = 14.8/Re^{0.95} \quad (3)$$

• II. Reynolds numbers from 400 to 550:

A recirculation downstream of the wire is observed. This recirculation along with the azimuthal component of the flow in this area produces a helical flow which is similar to the one observed in wire coil W01 (Fig. 11). Increase of the friction factor goes from 25% at $Re = 400$ to 45% at $Re = 500$.

• III. Reynolds numbers from 550 to 750:

Oscillating central flow. At $Re = 550$ a smooth undulating flow is observed. At $Re = 600$, the flow remains laminar but the flow oscillations become more abrupt.

• IV. Reynolds numbers higher than $Re = 750$:

The flow is fully turbulent. From $Re = 750$ to $Re = 3000$ the friction factor is almost constant and similar to $f = 0.04$. A constant friction factor value implies that the pressure drop is proportional to the flow mean square of the mean flow velocity. This is typical for turbulent flow. From $Re = 3000$ on, the tendency is for the friction factor to become typical of flow in tubes with structured roughness ($f \propto Re^{-0.2}$).

3.4. Wire Coil W03, long pitch

This is a very long pitch wire coil with $p/d = 3.66$ (three times longer than wire coil W01). Features for the flow of this wire are different to those of the previous two wires. A separated flow is not produced. Instead the flow at the peripheral region follows an angle near to that of the helix.

Fig. 13 shows experimental results for the pressure drop for a Reynolds number range between 50 and 80 000. Next, results for the three flow patterns observed are commented upon:

• I. Reynolds numbers between 0 and 700:

Stable laminar flow. The flow of the wire region passes through the wire without any type of recirculation. Friction factor results in this region can be correlated by:

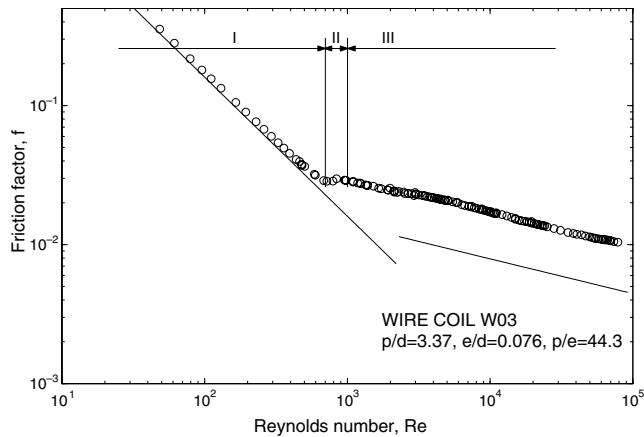


Fig. 13. Fanning friction factor vs. Reynolds number. Wire coil W03 results.

$$f = 13.3/Re^{0.97}. \quad (4)$$

At low Reynolds numbers ($Re = 200$) only azimuthal velocity components in a '1e' region downstream to the wire are observed. At $Re = 600$ this region of influence is of approximately '4e'.

Flow features are very similar to those of the laminar flow in a smooth tube, where the wire increases the pressure drop due mainly to the hydraulic diameter reduction. Fig. 14 shows a sketch of the flow pattern observed by the hydrogen bubble technique. Section A–A' shows that the flow finds an ellipse-shaped section. Since this is a much smoother shape than the circular one, flow separation is avoided.

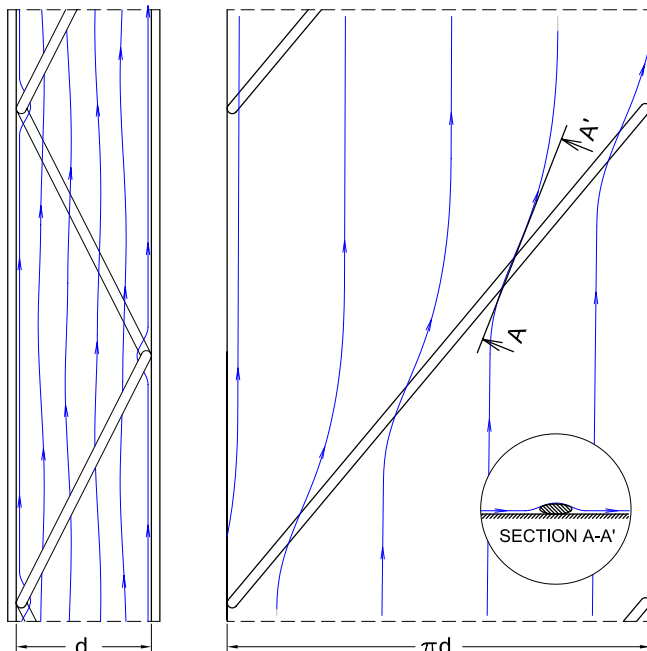


Fig. 14. Flow features for wire coil W03 at $Re < 700$. Left: central flow. Right: flow in the peripheral region.

• II. Reynolds numbers from 700 to 1000:

Oscillating central flow. At $Re = 700$ a small spiral downstream of the wire is observed. Its size is of the order of magnitude of the wire diameter. At $Re = 750$ a moderate flow oscillation is observed and at $Re = 850$ turbulence outbreaks start to appear. In this region the friction factor becomes constant at $f = 0.027$. Pressure drop stops being proportional to the mean velocity and becomes proportional to the square of mean velocity.

• III. Reynolds numbers higher than 1000:

The flow is fully turbulent. In this wire the friction factor changes from being 10% higher than the smooth tube at $Re = 700$ to being 110% higher at $Re = 3000$.

4. Conclusions

- (1) An analysis of the flow mechanism in tubes with wire coils using hydrogen bubble visualization and PIV techniques has been carried out. Results have been contrasted with the experimental results on pressure drop. The clear relation between the studied flow patterns and the friction factor has been analysed.
- (2) The experimental analysis allows one to establish that at low Reynolds numbers ($Re < 500$) the flow in tubes with wires is essentially similar to the flow in a smooth tube. Wire coils reduce the hydraulic diameter. This fact along with the light spin which wires cause in the central flow leads to a small increase in the friction factor.
- (3) Wires coils accelerate considerably the transition to the turbulence. This is produced at $Re_{crit} = 700$ in wire W01, at $Re_{crit} = 750$ in wire W02 and at $Re_{crit} = 1000$ in wire W03. Transition to turbulence is produced earlier in shorted-pitch wire coils.
- (4) Shorted-pitch wire coils cause the appearance of a separated flow at Reynolds numbers closer to 400. This recirculation together with the azimuthal velocity component produces a helical flow which ascends along the wire coil body. In the wire with the longer pitch W03 a flow separation does not take place. Due to the fact that the angle of the spiral of the wire is very small, the fluid near to the wall takes an oblique path to the wire and crosses an elliptical-shaped geometry. Since the fluid crosses a geometry that is not very rough, separation of the flow and recirculation downstream to the wire do not take place.
- (5) The current paper supplies data on physical flow behaviour in wire coils. This is an open question, just as was shown in previous works. The study carried out using three different wire coils describes the different flow patterns and their influence on the transition from laminar to turbulent flow.

Acknowledgement

This research has been partially financed by the DPI2003-07783-C02 grant of the “Dirección General de Investigación del Ministerio de Educación y Ciencia de España” and the “HRS Spiratube” company.

Appendix A. Supplementary data

Supplementary data associated with this article can be found, in the online version, at [doi:10.1016/j.ijheatfluidflow.2006.07.001](https://doi.org/10.1016/j.ijheatfluidflow.2006.07.001).

References

- Dewan, A., Mahanta, P., Sumithra Raju, K., Suresh Kumar, P., 2004. Review of passive heat transfer augmentation techniques. In: Proceedings of INSTN Mechanical Engineers. Part A: J. Power and Energy, vol. 218.
- García, A., Vicente, P.G., Viedma, A., 2005. Experimental study of heat transfer enhancement with wire coil inserts in laminar-transition-turbulent regimes at different Prandtl numbers. *International Journal of Heat and Mass Transfer* 48, 4640–4651.
- Inaba, H., Ozaki, K., Kanakoa, S., 1994. A fundamental study of heat transfer enhancement and flow-drag reduction in tubes by means of wire coil insert, Nippon Kikai Gakkai Ronbunshu. Transact. the Jpn Soci. Mech. Enginrs 60, 240–247.
- ISO, 1995. Guide to the expression of uncertainty in measurement, first ed., ISBN 92-67-10-188-9, International Organization for Standardization, Switzerland.
- Li, H.M., Ye, K.S., Tan, Y.K., Deng, S.J., 1982. Investigation on Tube-Side Flow Visualization, Friction Factors and Heat Transfer Characteristics of Helical-Ridging Tubes. In: Grigull, U. et al. (Eds.), *Heat Transfer 1982, Proceedings, Seventh International Heat Transfer Conference*, vol. 3. Hemisphere Publishing Corp., Washington, D.C., pp. 75–80.
- Ravigururajan, T.S., Bergles, A.E., 1994. Visualization of flow phenomena near enhanced surfaces. *Journal of Heat Transfer* 116, 54–57.
- Uttarwar, S.B., Raja Rao, M., 1985. Augmentation of laminar flow heat transfer in tubes by means of wire coil inserts. *Transactions of the ASME* 107, 930–935.
- Vicente, P.G., García, A., Viedma, A., 2002. Experimental study of mixed convection and pressure drop in helically dimpled tubes for laminar and transition flow. *International Journal of Heat and Mass Transfer* 45, 5091–5105.
- Vicente, P.G., García, A., Viedma, A., 2004. Mixed convection heat transfer and isothermal pressure drop in corrugated tubes for laminar and transition flow. *International Communications of Heat and Mass Transfer* 31, 651–662.
- Wang, L., Sundén, B., 2002. Performance comparison of some tube inserts. *International Communications of Heat and Mass Transfer* 29 (1), 45–56.